

Quantitative Analysis of QRS Detection Algorithms Based on the First Derivative of the ECG

Natalia M. Arzeno, Chi-Sang Poon, and Zhi-De Deng

Abstract—Accurate processing of electrocardiogram (ECG) signals requires a sensitive and robust QRS detection method. In this study, three methods are quantitatively compared using a similar algorithm structure but applying different transforms to the differentiated ECG. The three transforms used are the Hilbert transformer, the squaring function, and a second discrete derivative stage. The first two have been widely used in ECG and heart rate variability analysis while the second derivative method aims to explain the success of the Hilbert transform. The algorithms were compared in terms of the number of false positive and false negative detections produced for records of the MIT/BIH Arrhythmia Database. The Hilbert transformer and the squaring function both produced a sensitivity and positive predictivity of over 99%, though the squaring function had a lower overall detection error rate. The second derivative resulted in the highest overall detection error rate. Different algorithms performed better for diverse ECG characteristics; suggesting that an algorithm can be specified for different recordings, the algorithms can be combined based on each one's characteristics to determine a new more accurate method, or an additional detection stage can be added to reduce the number of false negatives.

Index Terms—Electrocardiography, Heart-rate variability, Hilbert transform, Peak detection

I. INTRODUCTION

THE basis for electrocardiogram (ECG) processing is the correct detection of the QRS complex. This complex, representing the depolarization of the left ventricle can identify the relative time segments of normal P- and T-waves while indicating the electrical progression in the heart with its shape. In addition, over the past decade heart-rate variability (HRV) analysis has become of interest as a tool for screening the existence and progression of diseases such as obstructive sleep apnea syndrome [1] and congestive heart failure [2]. However, the ECG recording may contain

Manuscript received April 3, 2006. This work was supported by National Institutes of Health Grants HL075014 and HL079503.

N. M. Arzeno (natalia2@mit.edu) is with the Department of Electrical Engineering and Computer Science, Massachusetts Institute of Technology, Cambridge, MA 02139 USA. She is recipient of an NIH undergraduate research training award HL075014-01S1.

Z.-D. Deng (zzzdeng@mit.edu) is with the Department of Electrical Engineering and Computer Science and the Department of Physics, Massachusetts Institute of Technology, Cambridge, MA 02139 USA. He contributed equally to this work.

C.-S. Poon is with the Harvard-MIT Division of Health Sciences and Technology, Massachusetts Institute of Technology, Cambridge, MA 02139 USA. (phone: 617-258-5405; fax: 617-258-7906; e-mail: cpoon@mit.edu).

problematic areas such as segments with high noise content, sudden changes in the QRS amplitude, or muscle and electrode artifacts which are not often detected correctly [3]. Multiple artifacts in the beat-to-beat interval (RRI) signal have been shown to increase its spectral power at all frequencies, motivating the need for a peak detector with minimal detection error [4].

Automatic QRS detection is necessary for the processing of long ECG recordings such as nighttime data or 24-hour Hoelter recordings. Though many approaches exist in QRS detection algorithms, this study concentrates on processing the first derivative of the ECG, exploiting the idea that the QRS complex is represented as a high-frequency feature of the ECG. First-derivative-based detection methods are often used in real-time analysis since they do not require extensive computations; however, avoiding a delay in the detection has also shown to increase the detection error [5], [6]. Another fast and accurate detection method sums the differentiated ECGs from different leads and then compares the result to three different thresholds [7]. This method has the disadvantage of requiring at least two recording leads, thus being more inconvenient for the patient and more memory intensive than single lead recordings. The algorithms in this study are designed for HRV analysis, contain data from only one ECG lead at a time, and are compared in terms of detection errors rather than computational efficiency. The first two algorithms, based on the Hamilton-Tompkins algorithm [8] and the use of the Hilbert transform [9], have been widely used in HRV analysis whereas the third algorithm, based on the second derivative of the ECG, aims to better explain the accuracy of that based on the Hilbert transform.

II. METHODOLOGY

A. Algorithm Structure

Three QRS detection algorithms were tested on the 48 ECG recordings of the MIT-BIH Arrhythmia Database [10]. As in previous studies, ventricular flutter episodes were eliminated in Record 207 [8], [9]. The 30-minute recordings were sampled at 360 Hz with 11-bit resolution over a 10 mV range. The three methods followed the same general structure, differing in the transform that was applied to the differentiated signal. The three transforms used were: Hilbert transformer, squaring function, and discrete differentiation. The ECG signal was processed with a bandpass filter (BPF) and a backward differentiation stage. The Kaiser Window

BPF had a passband of 8-20 Hz [9]. The filter provided attenuation of high-frequency noise and baseline shift, and the P- and T-waves were attenuated by the differentiation, providing a signal with outstanding peaks as an input to the transform. The transform was applied to a moving 1024-point window and compared to a variable threshold. The largest amplitude within a 200 ms window of each identified peak in the transform was stored for further consideration. The 200 ms window was set by the refractory period where the heart is not capable of beating more than once. A search-back mechanism identified the real peaks by finding the maximum in the ECG within ± 10 samples of the detected peak in the transform output. The procedure is illustrated in Fig. 1.

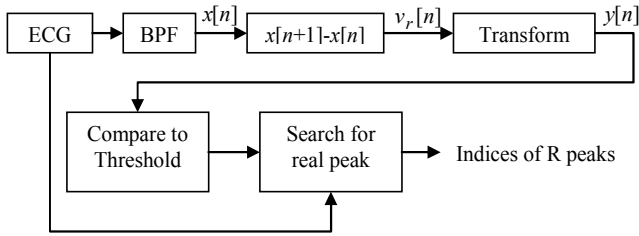


Fig. 1. Structure of Peak Detection Algorithms.

The threshold was determined as follows: The root mean squared (RMS) value of the 1024-point signal was calculated, and if it was larger than 18% of the maximum value, the threshold was set to be 39% of the maximum value of the segment. If the maximum value was in turn larger than twice the maximum value of the previous segment, the threshold was raised to 39% of the maximum value of the previous segment. If the RMS of the segment was less than 18% of its maximum value, the threshold was set to 1.6 times the RMS value [9]. Since the transform output of the second derivative method contains downward peaks, the threshold determination maxima become minima and peaks are identified if they are below the threshold.

B. Method I. Hilbert Transform.

The QRS detection method proposed by Benitez *et al.* [9] was followed in the analysis of the signals. The applied transform—the Hilbert transformer—is an odd-phase, ideally all-pass filter. Thus the zero-crossings in the ECG derivative due to the QRS complexes become peaks before being compared to the threshold.

The Hilbert transform provides a relationship between the real and imaginary parts of a signal. The algorithm was implemented in MATLAB, taking the real part of the signal to be the differentiation of the ECG ($v_r[n]$), constructing the corresponding analytic signal ($v[n]$) and then taking the imaginary part as the Hilbert signal ($v_i[n]$). The calculation of the analytic signal can be seen in (1) where Fast Fourier Transform (FFT) of the real part is multiplied with a vector of the same length with 1s at the zero and Nyquist frequencies and 2s in every other position. The inverse FFT

of the product corresponds to the analytic signal. The relationships between the variables are as follows [11]:

$$V(e^{j\omega}) = \begin{cases} 2V_r(e^{j\omega}), & 0 < \omega < \pi \\ V_r(e^{j\omega}) & \omega = 0, \pi \\ 0 & -\pi < \omega < 0 \end{cases} \quad (1)$$

$$V_i(e^{j\omega}) = \begin{cases} -jV_r(e^{j\omega}), & 0 < \omega < \pi \\ jV_r(e^{j\omega}) & -\pi \leq \omega < 0 \end{cases} \quad (2)$$

$$V_i(e^{j\omega}) = H(e^{j\omega})V_r(e^{j\omega}) \quad (3)$$

$$H(e^{j\omega}) = \begin{cases} -j, & 0 < \omega < \pi \\ j, & -\pi < \omega < 0 \end{cases} \quad (4)$$

From (3) and (4), the differentiated ECG is equivalently put through an all-pass filter—the Hilbert transformer—with frequency response of -90° shift for positive frequencies and $+90^\circ$ shift for negative frequencies. The output of the transform is the imaginary part of the analytic signal:

$$y[n] = v_i[n]. \quad (5)$$

Because it is an odd filter, the zero-crossings of the differentiated ECG, which correspond to the R-peaks, will be represented as peaks in the output of the transform.

C. Method II. Hamilton-Tompkins Algorithm.

The second detection algorithm, based on that described by Hamilton and Tompkins [8] implemented a squaring function as the transform:

$$y[n] = v_r[n]^2. \quad (6)$$

Since the original algorithm was based on real-time detection and this study aimed to process recorded signals, the peak was not detected based on its slope but rather using the maxima detector previously described. The square of the derivative provided peaks with increased magnitude in the location of the QRS complexes and further attenuation of the other ECG features. The transform can also be viewed as a measurement of energy where the threshold verifies if the output is enough to carry the energy of a QRS complex, proving to be the only method where the polarity of the QRS complex is irrelevant [5].

Method II, contrary to the other algorithms, included a secondary threshold to test for missed peaks. This secondary threshold [8] was implemented if the current RRI exceeded 1.5 times the previous RRI. The secondary threshold was 0.3 times the current threshold to the RRI, thus detecting peaks that were not originally above threshold. The secondary threshold is only applied to this algorithm due to its nonlinear scale. By squaring the differentiated ECG, peaks with small magnitude as well as wide arrhythmic peaks with decreased slope are reduced in the output of the transform. Yet these peaks are not attenuated as much as noise or other features of the ECG, allowing for the secondary threshold to be implemented. The secondary threshold cannot be implemented for the other methods since the small or wide peaks

will be at comparable magnitudes to the noise and other waves at the output of the transform.

D. Method III. Second Derivative.

The third detection algorithm aimed to test if the success of Method I was based on passing the differentiated ECG through an odd filter, or if some other characteristic of the Hilbert transformer was responsible for its success in previous studies. The transform for Method III was a second stage of differentiation:

$$y[n] = v_r[n] - v_r[n-1]. \quad (7)$$

The second differentiator stage ($D(e^{j\omega})$) presented a filter with odd phase and non-unity frequency response:

$$D(e^{j\omega}) = 1 - e^{-j\omega}, \quad (8)$$

$$|D(e^{j\omega})| = \sqrt{2 - 2\cos(\omega)}. \quad (9)$$

The algorithm introduced an additional high-pass filtering stage, contrary to the all-pass filtering stage from Method I.

E. Algorithm Comparison.

The three algorithms were compared by calculating the number of false positives (FP), true positives (TP) and false negatives (FN) for each record [12]. The Sensitivity (Se) and Positive Predictivity (+P) of each method were calculated. These statistics are defined as:

$$\text{Sensitivity} = \frac{TP}{TP + FN}, \quad (10)$$

$$\text{Positive predictivity} = \frac{TP}{TP + FP}. \quad (11)$$

The average time error between the real and detected peaks was also calculated [9]:

$$\text{Average Time error (ms)} = \frac{\sum | \text{Detected QRS time} - \text{Actual QRS time} |}{TP}. \quad (12)$$

III. RESULTS

The three algorithms resulted in comparable total Se and +P values for the 48 records of the MIT/BIH arrhythmia database, as can be seen in Table I. The secondary threshold was tested on Method I, but provided 88.54% +P for the first ten records and was thus discarded as a potential improvement on the algorithm.

TABLE I
CUMULATIVE RESULTS FOR PEAK DETECTION

Method	FP	FN	Se (%)	+P (%)	Error (ms)
I	745	928	99.08	99.26	7.43
II	727	661	99.40	99.34	6.71
III	872	2128	97.90	99.13	6.91

All of the algorithms produced values of Se and +P below 99%. The number of records for which this occurred and the

minimum values of Se and +P for each algorithm are listed in Table II. The records with low +P or Se are characterized in Section IV.

TABLE II
LOW SENSITIVITY AND POSITIVE PREDICTIVITY

Method	Se < 99%	Min Se (%)	+P < 99%	Min +P (%)
I	8	93.77	10	89.59
II	8	95.84	11	91.3
III	16	80.26	10	86.39

IV. DISCUSSION

Method II, based on the Hamilton-Tompkins algorithm, resulted in the minimum total number of FPs and FNs. Method I, also produced a Se and +P above 99%. The difference in Se between Methods I and II can be understood by the nature of the algorithms where the secondary threshold applied to Method II reduces its FNs though it slightly increases the number of FPs for areas with low signal-to-noise ratio (SNR). Method III proved to have similar results to Method I, but with a higher error rate, suggesting odd filters with diverse magnitude characteristics will perform differently as peak detectors. Though the results of Methods I and II were not strikingly different, each one fails at specific instances in the ECG recordings. The outstanding failures for the algorithms were due to:

1. negative QRS complexes
2. low-amplitude QRS complexes
3. wide premature ventricular contractions (PVCs)
4. low SNR

In this study, the algorithms had increased FPs when the polarity of the QRS complex was reversed. They also failed at detecting these peaks in the correct location due to the maxima detector in the algorithm. Method II, however, performed the best in these cases since the positive peaks in the transform output corresponded to the QRS complexes whereas Methods I and III had reversed peaks at the transform output, resulting in worsened detection. Five records contained negative QRS complexes amongst the positive ones, resulting in values of Se and +P below 99%.

Low-amplitude QRS complexes were mainly present in one record. The low-amplitude prevented the QRS complexes from having a positive slope large enough to be detected by Methods I and III. Method II, however, correctly detected the low-amplitude peaks with the secondary threshold, presenting yet another advantage of this algorithm.

Wider peaks, corresponding to arrhythmic beats, occurred more frequently than the first two failure instances, presenting the main advantage of Method II by making use of its secondary threshold. Record 208 contained uniform PVCs which were not detected correctly with Methods I and III as seen in Fig. 2. Method III (Fig. 2d) had the highest failure rate of the algorithms, resulting in false negatives for almost all of the PVC. Method I (Fig. 2b) had less of a difference between the normal beats (marked as *) and the

ectopic beats (marked as \wedge) in the transform output which was compared to the threshold. The secondary threshold for Method II (Fig. 2c) allowed for the detection of more PVCs than the other algorithms, though it still did not result in perfect detection. Similar results were observed for four additional records.

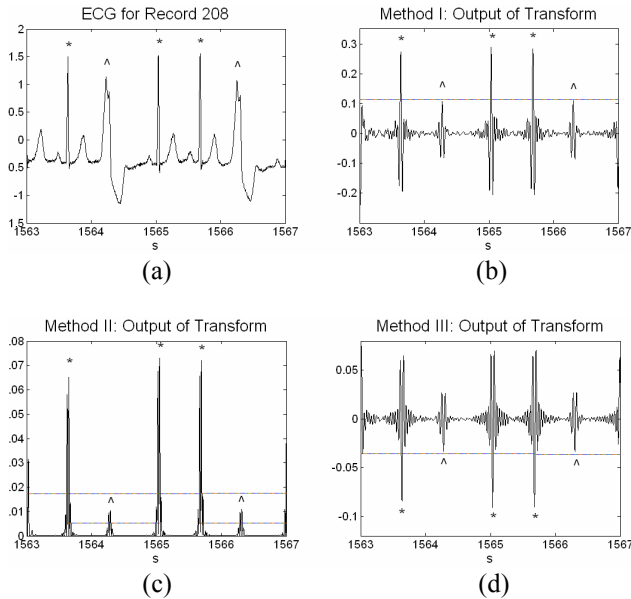


Fig. 2. PVC in Record 208. A segment of the original ECG and the outputs of the transforms are plotted. The * signals a normal beat and the \wedge signals a PVC. The horizontal lines in the transform outputs show where the threshold was set for each 1024-pt window. The lower lines in Method II represent the secondary threshold.

The secondary threshold in Method II slightly increases the detection error for signals with low SNR. Though all of the algorithms produced FPs for two records with low SNR, Method II had the largest number of false detections for these records. Without the secondary threshold, Method II resulted in near perfect detection, indicating a flaw of the secondary threshold. Methods I and III yielded fewer FPs than Method II for the records with low SNR, thus having better performance for signals with high noise content.

Since the algorithms are based on the first derivative of the ECG, wide beats and small QRS complexes present the major detection challenge. The secondary threshold resolves some of the discrepancies in Method II, yet it also presents a disadvantage in signals with high noise content since some of the noise gets falsely detected. Though only two records in this study were characterized with a significant amount of noise mistaken as beats, additional steps can be taken to correct these FPs. One such addition could be a stage that compares the amplitude of the detected beat in the ECG with the previous detected R peaks. Recordings with the mentioned features not detected by the algorithms will have RRI plots with outstanding peaks. Beats in these areas can be

detected with a kind of peak detection modified for arrhythmic beats or revised by an expert to extract the real peaks if an optimal algorithm cannot be applied.

V. CONCLUSION

Two of the three algorithms presented in this study—Methods I and II—resulted in Se and +P above 99%, where the high detection rate depends greatly on the chosen threshold. The results of Method III suggest the success of the Hilbert transform is partially due to the odd-phase component of the filter but detection is improved by its uniform magnitude. Since Methods I and II perform differently for certain ECG features such as PVCs or low SNR, a combination of the two algorithms could be taken to form an even better detection system. Alternatively, the algorithms could be used as a primary detection system, and outstanding values in the beat-to-beat intervals can be resolved depending on the application.

REFERENCES

- [1] L. Zapanta, C.-S. Poon, D.P. White, C.L. Marcus, E.S. Katz. Heart Rate Chaos in Obstructive Sleep Apnea in Children. *IEEE Trans. Eng. Med. Biol.*, 6:3889-92, 2004.
- [2] C.-S. Poon, C. Merrill, "Decrease of cardiac chaos in congestive heart failure". *Nature*, 389:492-495, 1997.
- [3] B.-U. Kohler, C. Hennig, R. Orlgemeister, The Principles of Software QRS Detection. *IEEE Trans. Eng. Med. Biol. Mag.* 21(1):42-57, 2002.
- [4] G. Berntson, J. Stowell, ECG artifacts and heart period variability: Don't miss a beat!. *Psychophysiology*, 35:127-132, 1998.
- [5] S. Suppappola, Y. Sun. Nonlinear Transforms of ECG Signals for Digital QRS Detection: A Quantitative Analysis. *IEEE Trans. Biomed. Eng.*, 41(4): 397-400, 1994.
- [6] M. Paoletti, C. Marchesi. Discovering dangerous patterns in long-term ambulatory ECG recordings using a fast QRS detection algorithm and explorative data analysis. *Computer Methods and Programs in Biomedicine*, 82(1):20-30, 2006.
- [7] I. Christov. Real time electrocardiogram QRS detection using combined adaptive threshold. *BioMedical Engineering OnLine*, 3:28, 2004.
- [8] P.S. Hamilton, W.J. Tompkins. Quantitative Investigation of QRS Detection Rules Using the MIT/BIH Arrhythmia Database. *IEEE Trans. Biomed. Eng.*, 12:1157-1165, 1986.
- [9] D. Benitez, P.A. Gaydecki, A. Zaidi, A.P. Fitzpatrick. The use of the Hilbert transform in ECG signal analysis. *Computers in Biology and Medicine*, 31:399-406, 2001.
- [10] A.L. Goldberger, et al. PhysioBank, PhysioToolkit, and PhysioNet: Components of a New Research Resource for Complex Physiologic Signals. *Circulation* 101(23):e215-e220 [Circulation Electronic Pages; <http://circ.ahajournals.org/cgi/content/full/101/23/e215>]; 2000
- [11] A.V. Oppenheim, R.S. Schaffer. Discrete-Time Signal Processing. Prentice-Hall, Englewood Cliffs, NJ, 2nd ed. 1999.
- [12] American National Standard for Ambulatory Electrocardiographs, publication ANSI/AAMI EC38-1994, Association for the Advancement of Medical Instrumentation, 1994.
- [13] J. Pan, W. Tompkins. A Real-Time QRS Detection Algorithm. *IEEE Trans. Biomed. Eng.*, 32(3):230-236, 1985.
- [14] V.X. Alfonso, W.J. Tompkins, T.Q. Nguyen, S. Luo. ECG Beat Detection Using Filter Banks. *IEEE Trans. Biomed. Eng.*, 46(2):192-202, 1999.
- [15] W.H. Chang, K.-P. Lin, S.-Y. Tseng. ECG Analysis on Hilbert Transform Description. *IEEE Trans. Eng. Med. Biol.* 1988.
- [16] D.S. Benitez, P.A. Gaydecki, A. Zaidi, A.P. Fitzpatrick. A New QRS Detection Algorithm Based on the Hilbert Transform. *Computers in Cardiology*, 27:379-382, 2000.